Plant Physiology Preview. Published on November 7, 2011, as DOI:10.1104/pp.111.184333

Response of Diatom C Metabolism to N Starvation

Corresponding Author
Gill Malin
Laboratory for Global Marine and Atmospheric Chemistry
School of Environmental Sciences
University of East Anglia
Norwich Research Park
Norwich
NR4 7TJ
UK
+44 1603 592531
g.malin@uea.ac.uk

Journal research area: Environmental Stress and Adaptation

The Response of Diatom Central Carbon Metabolism to Nitrogen Starvation is Different to that of Green Algae and Higher Plants

Nicola Louise Hockin[ac], Thomas Mock[b], Francis Mulholland[d], Stanislav Kopriva[c] and Gill Malin[a]

[a] Laboratory for Global Marine and Atmospheric Chemistry, School of Environmental Sciences, University of East Anglia, Norwich Research Park, Norwich, NR4 7TJ, UK

[b] School of Environmental Sciences, University of East Anglia, Norwich Research Park, Norwich, NR4 7TJ, UK

[c] John Innes Centre, Norwich Research Park, Colney, Norwich, NR4 7UH, UK

[d] Institute of Food Research, Norwich Research Park, Colney, Norwich, NR4 7UA, UK

Footnotes

This work was supported by a Norwich Research Park Studentship and by the John Innes Centre and University of East Anglia Earth & Life Systems Alliance. G.M. was funded through a UK Natural Environment Research Council Advanced Fellowship (NE/B501039/1) and S.K is supported by the UK Biotechnology and Biological Sciences Research Council.

Abstract

The availability of nitrogen varies greatly in the ocean and limits primary productivity over large areas. Diatoms, a group of phytoplankton that are responsible for about 20% of global carbon fixation, respond rapidly to influxes of nitrate and are highly successful in upwelling regions. Although recent diatom genome projects have highlighted clues as to the success of this group, very little is known about their adaptive response to changing environmental conditions. Here we compare the proteome of the marine diatom *Thalassiosira pseudonana* (CCMP 1335) at the onset of nitrogen starvation with that of nitrogen replete cells using 2-dimensional gel electrophoresis. In total 3310 protein spots were distinguishable and we identified 42 proteins increasing and 23 decreasing in abundance (fold change >1.5, P <0.005). Proteins involved in the metabolism of nitrogen, amino acids, proteins and carbohydrates, photosynthesis and chlorophyll biosynthesis were represented. Comparison of our proteomics data to the transcriptome response of this species under similar growth conditions showed good correlation and provided insight into different levels of response. The *T. pseudonana* response to nitrogen starvation was also compared to that of the higher plant *Arabidopsis thaliana*, the green alga *Chlamydomonas reinhardtii* and the cyanobacterium *Proclorococcus marinus*. We have found that the response of diatom carbon metabolism to nitrogen starvation is different to that of other photosynthetic eukaryotes and bears closer resemblance to the response of cyanobacteria.

Introduction

Nitrogen is an essential nutrient for all organisms and is required for the biosynthesis of macromolecules, such as proteins, nucleic acids and chlorophyll. The availability of nitrogen in the ocean varies dramatically on spatial and temporal scales due to physical and biological processes. As for terrestrial plants, nitrogen is a major limiting nutrient for primary production in the ocean, with consequences for marine food webs (Falkowski 1997).

Diatoms, characterised by their silica frustules, are a key group of the eukaryotic phytoplankton and are found throughout the world's oceans from polar to tropical latitudes. This group is particularly successful in upwelling environments, where they are able to rapidly respond to nitrate influx and out-compete other marine phytoplankton while this nutrient and silicate are abundant (Estrada and Blasco 1979). As much as 20% of global net primary productivity can be accounted for by diatoms, which is more than all terrestrial rainforests combined (Nelson et al. 1995; Field et al. 1998), and the sheer magnitude of their productivity in upwelling regions provides the basis of short, energy-efficient food webs that support large scale coastal fisheries (Mann 1993). Diatoms are also important contributors to biological carbon pump that draws carbon down into the deep ocean through the settling of cells.

Diatoms belong to the heterkont algae, which arose from a secondary endosymbiotic event when a photosynthetic eukaryote, thought to be a red alga, was engulfed by a heterotrophic eukaryotic host (Falkowski et al. 2004). The pathway of nitrate assimilation in diatoms is comparable to that of other eukaryotic photoautotrophs (Armbrust et al. 2004; Bowler et al. 2008) and there is evidence that some elements are of endosymbiont origin (Bowler et al. 2010).

Nitrate is taken up into the diatom cell, where it is first reduced to nitrite by a cytosolic NADH-dependent nitrate reductase (NR) (Gao et al. 1993; Berges and Harrison 1995; Allen et al. 2005). Nitrite is then transported into the chloroplast and further reduced to ammonium by a cyanobacterial-like ferredoxin-dependent nitrite reductase (Fd-NiR) (Milligan and Harrison 2000; Bowler et al. 2010). The joint action of glutamine synthetase (GS) and glutamate synthase (GOGAT) is thought to be the main route of ammonium assimilation into amino acids and other nitrogenous compounds (Dortch et al. 1979; Clayton and Ahmed 1986; Zehr and Falkowski 1988). Diatoms possess a plastid localised glutamine synthetase II (GSII) that is of red algal origin (Robertson et al. 1999; Robertson and Tartar 2006; Siaut et al. 2007) and thought to be responsible for the assimilation of ammonium produced by nitrate reduction. Transcript levels of *glnII* (encoding GSII) are higher in diatom cells assimilating nitrate than in those assimilating ammonium directly (Takabayashi et al. 2005). Diatoms

appear to have an NADH-dependent glutamate synthase (NAD(P)H-GOGAT) and also a ferredoxin-dependent (Fd-GOGAT) form for this enzyme, that is thought to be plastid localised (Clayton and Ahmed 1986; Zadykowicz and Robertson 2005), however our knowledge on this enzyme is limited. The activity of the GS/GOGAT cycle requires input of carbon skeletons in the form of 2-oxoglutarate, while oxaloacetate is also important in the production of amino acids. These are both intermediates of the tricarboxylic acid (TCA) cycle and provide an important link between nitrogen assimilation and carbon metabolism.

A number of genes of bacterial origin have been identified in diatom genomes (Armbrust et al. 2004; Bowler et al. 2008) and these are thought to have been acquired by horizontal transfer (Allen et al. 2006). They include a cytosolic NAD(P)H-dependent nitrite reductase (NAD(P)H-NiR) which is homologous to nirB of bacteria and fungi, along with a mitochondrial glutamine synthetase III (GSIII) (Robertson and Alberte 1996; Armbrust et al. 2004; Allen et al. 2006; Siaut et al. 2007). Neither of these enzymes has been found in green algae or plants. Genome projects have also revealed that diatoms possess a full urea cycle (Armbrust et al. 2004; Bowler et al. 2008), which had not been found previously in eukaryotes outside the Metazoa. This pathway is thought to be involved in mobilising nitrogen and carbon produced by cell processes back into central metabolism (Allen et al. 2006). The presence of other bacterial-like genes in the diatom genome, such as an ornithine cyclodeaminase, which catalyses the conversion ornithine to proline in arginine degradation, might expand the function of the urea cycle (Bowler et al. 2010).

Diatoms have an evolutionary history, which is distinct from plants and green algae and this has brought together a unique combination of genes, providing the potential for novel biochemical processes in this group. Although genome and proteome studies offer clues as to the success of diatoms (Armbrust et al. 2004; Bowler et al. 2008; Nunn et al. 2009), further investigation is now required to understand the adaptive responses of diatoms to dynamic environmental conditions such as nutrient availability.

Here we compare the proteome of the diatom *Thalassiosira pseudonana* (CCMP 1335) at the onset of nitrogen starvation to that of nitrogen replete cells with the aim of gaining insight into the global regulation of metabolic pathways in response to nitrogen starvation. We assess our dataset alongside the results of a whole genome tiling-array analysis of *T. pseudonana* (CCMP 1335) in which the response to a comparable nitrogen starved condition was measured in a study of biosilification (Mock et al. 2008). This enables us to obtain a more detailed picture of the processes affected by nitrogen starvation in diatoms, and also gain insight into the levels of their regulation. In addition, through

comparison of our findings to higher plants, green algae and cyanobacteria, we demonstrate that the distinct evolutionary history of the diatoms has resulted in a fundamentally different metabolic response to nitrogen starvation compared to other eukaryotic photoautotrophs studied to date.

Results and Discussion

Physiological Effects of Nitrogen Deprivation

The onset of nitrogen starvation in *T. pseudonana* cultures grown with an initial nitrate concentration of 30 µM was identified by comparing daily cell counts and Fv/Fm values to nitrogen replete cultures grown with an initial nitrate concentration of 550 µM. Cultures grown with 30 µM nitrate were yield-limited by nitrogen availability at a maximum density of ca. 1 x 10^6 cell ml^{-1} on day 4 of the experiment, whereas cultures with 550 µM nitrate continued to grow to ca. 3 x 10^6 cell ml^{-1}. From day 3 to 5 the growth rate of low nitrate cultures was 0.21 d^{-1} compared to a growth rate of 0.51 d^{-1} in the nitrogen replete control cultures. The efficiency of photosystem II (Fv/Fm) of the low nitrate cultures decreased as growth became yield-limited. Fv/Fm was 0.57 in low nitrate cultures on day 4 compared to 0.63 in the nitrogen replete cultures and continued to decline, relative to that of nitrogen replete cultures, throughout the experiment (fig. S1).

Intracellular levels of nitrogenous molecules, such as free nitrate, amino acids and protein give a good indication of the nitrogen status of the cell. As the growth of the low nitrate cultures became yield-limited (day 4), levels of free nitrate and free amino acids were 3-fold lower than in the nitrogen replete control cultures (fig.1) and protein content was 2.2-fold lower. For the purpose of this study this point is considered to be the onset of nitrogen starvation. Furthermore, assuming a total nitrogen content of 1 pg per *T. pseudonana* cell (Berges et al 2002 and S. Chollet, University of East Anglia, personal communication), we calculate that, based on cell numbers, the medium of the low nitrate cultures would have been completely depleted of nitrate and that to support the cell density achieved the total cell nitrogen must be reduced, as suggested by the decline in the cellular content of nitrogenous compounds reported.

Proteome Comparison

Proteins are the biochemically active components that define the flux through metabolic pathways. Therefore, monitoring changes in their abundance provides good insight into how the cell is adapting to a specific condition. Here the proteomes of *T. pseudonana* cultures at the onset of nitrogen starvation were compared to those of nitrogen replete cultures using 2-dimensional gel electrophoresis

(fig. 2). Following filtering to remove speckling and background 3310 distinct protein spots were detected and taken for further analysis, of which 146 spots had a greater than 1.5-fold increase or decrease in relative abundance between the two treatments ($P<0.005$, based on t-test). These were picked from the gel and their MALDI-TOF MS analysis after trypsin digestion resulted in the identification of 94 spots belonging to 65 unique proteins, of which 42 were increased and 23 decreased at the onset of nitrogen starvation (table S1). Several of these proteins were present as multiple spots (fig. 2), most probably due to post-translational modifications, such as phosphorylation affecting the isoelectric point (pI) of the proteins. It should also be noted that not all regulated proteins can be identified using this kind of analysis. For example 2-dimensional gels are not optimised for membrane bound proteins and very low abundance proteins might also not be detected. Also, if the protein mass or pI were outside the range of the gel the protein would not be seen. While a broader pH range was tested (data not shown), we found that pH 4-7 gave the best spot separation and the maximum number of spots detected (fig. 2). The lack of identification of a specific protein thus does not prove its stable abundance under the growth conditions tested.

Functional Characterisation of Proteins

We were interested in the biological significance of changes in relative protein abundance associated with the onset of nitrogen starvation and proteins were therefore grouped according to the KEGG (Kyoto Encyclopedia of Genes and Genomes) categorisation (fig. 3). Proteins involved in nitrogen and protein metabolism decreased in abundance along with those of photosynthesis and chlorophyll biosynthesis. Carbohydrate and amino acid metabolism were highly represented in both the increasing and decreasing groups of proteins, making these processes potentially important in the adaptation of the cells to nitrogen starvation.

In an independent study on diatom silicon processing Mock et al (2008) compared the transcriptomes of the same *T. pseudonana* isolate grown under comparable, nitrogen starved and control, growth conditions by whole-genome tiling array. By assigning the same KEGG categorisation as described above to differentially regulated transcripts under nitrogen starvation (fold change>2, $P<0.05$) we demonstrate that the functional categories represented by differentially regulated transcripts (Mock et al 2008) are similar to those of the proteins described in the present study (fig. 3).

Nitrogen Assimilation

Proteins involved in the reduction of nitrate and nitrite to ammonium, such as NR (ProtID 25299), NADPH-NiR (ProtID 26941) and Fd-NiR (ProtID 262125) decreased by 2.5- to 9.5-fold in abundance in *T. pseudonana* at the onset of nitrogen starvation (fig. 4; table 1). Mock et al (2008), however,

detected no change in the transcript levels of genes encoding these proteins under comparable growth conditions, indicating post-transcriptional regulation of protein accumulation. Indeed, NR is known to be under multiple levels of regulation in diatoms as in other photosynthetic eukaryotes (Vergara et al. 1998; Parker and Armbrust 2005). Using GFP fused promoter and terminator elements, it has been demonstrated that the transcript levels of *nia* (encoding NR) are maintained under nitrogen limited conditions in the diatom *Cylindrotheca fusiformis*, but that nitrate is required for its translation (Poulsen and Kroger 2005). The decreased abundances of Fd- and NAD(P)H-NiR and the lack of change in transcript levels of the corresponding genes implies that they might be under similar regulation.

Despite a decrease in the abundance of proteins for nitrate and nitrite reduction, members of the GS/GOGAT cycle increased in abundance. We measured a 1.6- and 2.2-fold increase in GSIII (ProtID 270138) and NAD(P)H-GOGAT (ProtID 269160) abundance respectively. GSIII is not thought to contribute to the assimilation of ammonium derived from nitrate reduction since *glnN* (encoding GSIII) does not follow the diurnal expression pattern of genes involved in nitrate assimilation (NR, Fd-NiR and GSII) in the diatom *Skeletonema costatum* (Brown et al. 2009). Interestingly, GSIII is also induced in the cyanobacterium *Synechococcus* during the early stages of nitrogen deprivation (Sauer et al. 2000). In addition, Mock et al (2008) measured increased transcript levels of two NAD(P)H-GOGAT genes (ProtIDs 29861 and 269160) along with a ferredoxin-dependent form of this enzyme (ProtID 269900). Increased capacity for ammonium assimilation thus appears to be important in the response of *T. pseudonana* to nitrogen starvation. There has been limited research into diatom GOGAT isoforms, but it seems possible that NAD(P)H-GOGAT and GSIII might act together in the assimilation of ammonium produced by cellular processes, such as protein catabolism under this growth condition.

Diatoms possess a complete urea cycle, which may allow more efficient use of alternative nitrogen sources taken up and produced by cellular processes. The increased abundance of a urease (ProtID 30193) was seen in the present study, which could enable the cell to use urea as a nitrogen source in a reaction that yields ammonium. However, this protein spot coincided with another protein in the gel making it impossible to calculate an accurate fold-change. Mock et al (2008) found decreased transcript levels of a carbamoyl phosphate synthase (ProtID 40323), which directs ammonium into the urea cycle (Mock et al. 2008). This is in agreement with an increase in transcript level of carbamoyl phosphate synthase with the resupply of nitrogen to nitrogen starved *Phaeodactylum tricornatum* (Allen et al. 2011). Despite the decrease in transcript levels of this key enzyme of the urea cycle, an N-acetylornithine aminotransferase (ProtID 270136) and an N-acetyl-gamma-glutamyl-phosphate

reductase (21290), also members of this pathway, increased in protein abundance. These enzymes are considered to be involved in ornithine, and therefore arginine, biosynthesis and their increase might represent an up-regulation of this process. An upregulation in the production of ornithine may be a strategy to conserve reduced nitrogen since, unlike ammonium, this compound does not leak from the cell. Alternatively, under certain conditions these enzymes might function in the opposite direction and the enzyme acetylornithine aminotransferase has been shown to catalyse the transamination of ornithine in *Pseudomonas aeruginosa* and *Pseudomonas putida* in the catabolism of arginine (Voellmy and Leisinger 1975). The up-regulation of these enzymes might be therefore correlated with the degradation of amino acids discussed above.

A urea transporter (ProtID 24250) and an amino acid transporter (ProtID 262236) also increased in transcript level, suggesting that *T. pseudonana* increases its capacity to take up these alternative forms of nitrogen when nitrate availability is limited. Any source of intra- or extracellular nitrogen must first be converted to ammonium before assimilation to amino acids and other nitrogenous compounds. This may explain why although nitrate assimilation decreases at the onset of nitrogen starvation, ammonium assimilation remains important.

Protein and Amino Acid Metabolism

There is evidence for the remobilisation and redistribution of intracellular nitrogen in *T. pseudonana* at the onset of nitrogen starvation. The cellular protein content of *T. pseudonana* decreased and correspondingly, the abundance of two ribosomal proteins (ProtIDs 21235 and 15259) and a translation factor (ProtID 269148) decreased by 1.8- to 3.1-fold in abundance, suggesting that protein biosynthesis was decreased. Mock et al (2008) found that the transcript levels of a number of aminoacyl-tRNA synthetases, which bind specific amino acids to be added to the polypeptide chain by the ribosome, decreased under nitrogen starvation in this species. Protein degradation may also be increased given that a serine carboxypeptidase (ProtID 15093) increased 2-fold in protein abundance, and transcript levels for this gene and a further three proteases (ProtIDs 16390, 17687 and 38360) also increased (Mock et al. 2008). On the other hand, four other proteases (ProtIDs 29314, 866, 1738 and 31930) decreased in transcript level (Mock et al. 2008); this may be a response to the reduced protein content of the cell or alternatively differential expression of proteases with different substrate specificities may play a regulatory role in the response of *T. pseudonana* to nitrogen starvation.

While the total free amino acid content of *T. pseudonana* decreased at the onset of nitrogen starvation the abundance of individual amino acids showed different responses to this growth condition (fig. 5). The steady-state levels of many amino acids decreased; notably the most abundant members such as

glutamate, histidine, aspartate and serine decreased by 2.9- to 22.8-fold, contributing substantially to the decrease of total amino acids seen. On the other hand, leucine, cysteine, isoleucine and valine increased by 2.1- to 5.4-fold.

Correspondingly, the proteomics and transcriptomics analyses provide evidence for increased amino acid catabolism; the most highly increased protein in the current study was a branched chain aminotransferase (ProtID 260934) which changed 6.4-fold. This enzyme catalyses the first step in the degradation of the amino acids valine, leucine and isoleucine. Transcript levels of this gene and one other branched chain aminotransferase (ProtID 20816) also increased (Mock et al. 2008). Valine, leucine and isoleucine degradation proceeds via a number of oxidation steps, ultimately yielding the TCA cycle intermediates acetyl- or succinyl CoA. The transcript levels of an alpha-keto acid dehydrogenase complex (ProtIDs 795, 32067 and 36291), and a short-chain acyl-CoA dehydrogenase (ProtID 269127) that catalyse steps of this pathway, also increased (Mock et al. 2008). The increased intracellular valine, leucine and isoleucine levels in *T. pseudonana* at the onset of nitrogen starvation could be responsible for triggering the up-regulation of genes encoding enzymes catalysing their degradation.

A class V aminotransferase (ProtID 22208), which may be involved in amino acid degradation, increased 1.9-fold in protein abundance. However, the transcript level of this gene decreased, as did a number of others involved in amino acid catabolism, including genes involved in glycine, serine and threonine metabolism and degradation (Mock et al. 2008). The cellular content of these amino acids decreased 3- to 4-fold at the onset of nitrogen starvation and may have reached such a level that transcription of genes involved in their degradation had ceased. The degradation of proteins and amino acids produces ammonium, which might be reassimilated by GS/GOGAT enzymes, as discussed above. Various carbon skeletons, many of which are also TCA cycle intermediates are also produced by this process (fig. 6).

It is noteworthy that intracellular levels of the amino acid proline decreased 2.5-fold in *T. pseudonana* at the onset of nitrogen starvation, since this is a major osmolyte in some marine diatoms (Dickson and Kirst 1987). Interestingly, we measured a 2.6-fold increase in intracellular dimethylsulphoniopropionate (DMSP), from 1.6 mM in nitrogen replete *T. pseudonana* cultures to 4.3 mM in cultures at the onset of nitrogen starvation. In addition to being the precursor of the environmentally important volatile sulphur compound, dimethylsulphide, DMSP is a compatible solute that does not contain nitrogen and Andreae (1986) suggested that it might replace nitrogen-containing osmolytes under nitrogen deprivation. Keller et al (1999) also found that DMSP increased

in *T. pseudonana* under nitrogen limited conditions, whilst the nitrogenous osmolytes including glycine betaine and amino acids were depleted. The proteins involved in the DMSP biosynthesis pathway have yet to be identified, although it is thought that the first step involves the transamination of methionine, to yield the 2-oxo acid 4-methylthio-2-oxobutyrate (MTOB) (Gage et al 1997). As discussed above, we identified a branched chain aminotransferase (ProtID 260934) as the most highly increased protein at the onset of nitrogen starvation and this may therefore be a candidate for the enzyme catalysing this step.

Photosynthesis

The down-regulation of photosynthesis is a universal response to nitrogen starvation among photosynthetic eukaryotes and accordingly we measured a reduction in the efficiency of photosystem II (Fv/Fm) in *T. pseudonana* under this growth condition. Carbon and nitrogen metabolism are closely linked, since the assimilation of nitrate to amino acids and nitrogenous compounds is an energy consuming process that requires reducing equivalents and carbon skeletons. Reduced nitrate assimilation causes excess of these components to accumulate, and the resultant metabolic imbalance leads to increased oxidative stress (Logan et al. 1999). Furthermore, photosynthetic carbon fixation requires nitrogen in proteins that facilitate electron transport and catalyse photosynthetic reactions. Lower protein content due to nitrogen starvation could therefore limit the flow of electrons though the photosynthetic apparatus, causing increased production of reactive oxygen species (ROS) and thus oxidative stress.

Chlorophyll is a nitrogenous macromolecule and reducing its synthesis reduces the nitrogen demand of the cells and also diminishes the light capturing capacity and ROS production. Therefore it is not surprising that five proteins involved in the synthesis of chlorophyll and its precursors decreased by 1.5- to 2.5-fold in abundance under nitrogen starvation; including a geranylgeranyl reductase (ProtID 10234), which has been shown to catalyse a critical step in chlorophyll synthesis in vascular plants (Tanaka et al. 1999). Transcript levels of six genes involved in chlorophyll biosynthesis (ProtIDs 32201, 26573, 32431, 5077, 262279 and 31012) were also found to decrease (Mock et al. 2008) and reduced chlorophyll content (Mock and Kroon 2002) and chlorophyll degradation (D. Franklin, personal communication) have previously been measured in *T. pseudonana* under nitrogen starvation.

In agreement with increased oxidative stress, a superoxide dismutase (ProtID 40713) and a mitochondrial alternative oxidase (ProtID 38428) both increased approximately 2.2-fold. The increase of intracellular levels of DMSP in *T. pseudonana* under nitrogen starvation might also be linked to oxidative stress. In addition to its role as a compatible solute DMSP is thought to be part of a cellular

antioxidant system (Sunda et al. 2002) and its synthesis and excretion might dissipate excess energy, carbon and reducing equivalents under nutrient limited conditions (Stefels 2000).

Carbon Metabolism

Reduced demand for carbon skeletons in nitrogen assimilation along with the production of carbon skeletons from catabolic processes, as described above, are expected to impact on central carbon metabolism. Indeed, in the proteome comparison we see evidence for increased glycolytic activity in *T. pseudonana* at the onset of nitrogen starvation that would direct carbon from intracellular carbohydrate stores to central carbon metabolism. The abundance of a phosphoglycerate mutase (ProtID 27850), enolase (ProtID 40391) and fructose-1,6-bisphosphate aldolase (ProtID 270288) increased by 1.5- to 2.9-fold (Fig. 6). Although these enzymes can also catalyse the reverse reactions of gluconeogenesis, transcript levels of a phosphofructokinase (ProtID 31232) and two pyruvate kinase genes (ProtIDs 22345 and 40393) also increased, while one pyruvate kinase (ProtID 4875) decreased (Mock et al. 2008). These enzymes are specific to glycolysis, indicating that this is the direction of carbon flow.

Pyruvate, the product of glycolysis, can be converted to acetyl CoA through the activity of the multi-enzyme complex pyruvate dehydrogenase. In our study the protein abundance of three subunits of this complex (ProtIDs 268374, 8778 and 268280) increased by around 2.0-fold. This enzyme is also unidirectional, further supporting an increase in glycolytic activity. Acetyl CoA is used in fatty acid biosynthesis and as a carbon input to the TCA cycle, which is a source of energy and reducing equivalents, but also provides carbon skeletons for nitrogen assimilation and the biosynthesis of compounds, including fatty acids. In this proteomics study many of the proteins of the TCA cycle increased by 1.6- to 2.5-fold in abundance (fig. 6), suggesting that the carbon from glycolysis might be channelled through acetyl CoA and then into this pathway.

Regulation

Regulating the balance between carbon and nitrogen metabolism is crucial, particularly under changing nitrogen availability, and there are a range of regulatory elements known to be involved in coordinating this response. The transcript levels of a number of other regulatory elements were altered in *T. pseudonana* at the onset of nitrogen starvation (Mock et al 2008). These include a NarL family histidine kinase (ProtID 24704), which increased in abundance, and also an alkaline phosphatase (ProtID 20880) and a phosphate transport system substrate binding protein (ProtID 262506), which both decreased in transcript level. These are all required for a two-component signal transduction pathway and might therefore act together in regulating the cell response to nitrogen starvation.

Inter-Species Comparison

This novel combined analysis of the proteome and transcriptome of *T. pseudonana* at the onset of nitrogen starvation has revealed that nitrate assimilation is reduced, which would reduce demand for energy, reducing equivalents and carbon skeletons, and in response photosynthetic carbon fixation is decreased. In higher plants and green algae photosynthetic carbon fixation is also reduced in response to nitrogen deprivation and excess carbon is generally stored in molecular pools that contain little or no nitrogen. In higher plants this is usually in the form of starch (Diaz et al. 2005; Wingler et al. 2006) and Peng et al (2007) described increased transcript levels of two genes involved in starch biosynthesis in *Arabidopsis thaliana* under nitrogen starvation. In the fresh water green alga *Chlamydomonas reinhardtii*, on the other hand, excess carbon is reportedly directed to fatty acid biosynthesis (Wang et al. 2009; Moellering and Benning 2010), and Miller et al (2010) found increased expression of genes involved in lipid biosynthesis in *C. reinhardtii* when nitrogen was not available. Diatoms are known to store carbon as chrysolaminaran (a β-1,3 glucan) or as lipids (Armbrust et al. 2004; Kroth et al. 2008), however proteins directly related to the synthesis or degradation of these compounds were not identified in the present study. The increase in glycolytic proteins and their transcripts in *T. pseudonana* seems opposed to the patterns described in higher plants and green algae; while they are increasing carbon stores, *T. pseudonana* appears to be remobilising them.

In addition, in both *A. thaliana* (Peng et al. 2007) and *C. reinhardtii* (Miller et al. 2010) transcript levels of genes associated with the TCA cycle either decreased in abundance or remained unchanged in response to nitrogen deprivation (fig. 7; table S2). This is very different to *T. pseudonana*, where the abundance of proteins and transcripts (Mock et al. 2008) associated with the TCA cycle increased at the onset of nitrogen starvation (fig. 6 and fig. 7). Comparison of proteins of the TCA that changed in abundance with changes in their transcript level under other growth conditions tested by Mock et al. (2008) (-Si, -Fe, -N, -CO_2 and decreased temperature) suggests that this response is specific to nitrogen starvation.

If photosynthetic carbon fixation is decreased in *T. pseudonana* due to reduced demand for carbon skeletons, reducing equivalents and energy, why are glycolysis and the TCA cycle, which are a source of these components, up-regulated? Interestingly a similar expression pattern, with increased levels of TCA cycle transcripts, is seen in the marine cyanobacterium *Prochlorococcus marinus* subsp. pastoris (strain CCMP1986, previously MED4) under nitrogen limited conditions (fig. 7) (Tolonen et al. 2006). These authors propose that under nitrogen limited conditions the breakdown of intracellular

stores is a more efficient source of carbon for the reassimilation of nitrogen than photosynthesis. As discussed above, photosynthesis is a nitrogen demanding process, which can also increase oxidative stress. This hypothesis fits with the proposed protein and amino acid catabolism and increased GS/GOGAT enzymes for ammonium assimilation seen in the current study. In common with cyanobacteria, diatoms possess a complete urea cycle (Armbrust et al. 2004), which has the potential to increase the efficiency of nitrogen reassimilation from catabolic processes (Allen et al. 2006) thereby leading to a higher demand for carbon skeletons than in organisms that lack a urea cycle. Changes in both protein abundance (table 1) and transcript levels of enzymes associated with the urea cycle were seen in *T. pseudonana* at the onset of nitrogen starvation. Allen et al. (2011) have demonstrated that in nitrogen starved *P. tricornatum* the urea cycle metabolites proline and urea are closely coupled to intermediates of the TCA cycle in their response to the addition of this nutrient. The authors propose that these pathways are linked through the aspartate-argininosuccinate shunt, as in animal cells, in which argininosuccinate is produced from aspartate dervived from oxaloactetate and citrulline. Argininosuccinate in turn is used in the production of arginine, with fumarate as a by-product that feeds back into the TCA cycle. Accordingly the effect of RNA interference-mediated knockdown of the key urea cycle enzyme carbamoyl phosphate synthase on fumarate and malate in this diatom was similar to that of urea cycle metabolites, while upstream TCA cycle intermediates were not as severely affected (Allen et al. 2011). In *T. pseudonana* at the onset of nitrogen starvation enzymes for fumarate and malate synthesis increased in abundance and this link between the urea and TCA cycles may therefore also have a role in the *T. pseudonana* response to nitrogen starvation. However, the transcript level and protein abundance of TCA cycle enzymes upstream of the aspartate-argininosuccinate shunt also increased in abundance suggesting that the TCA cycle may have additional or alternative functions in this response.

There are reports of increased lipid and fatty acid production in diatoms and many other microalgae under nitrogen starved conditions (Collyer and Fogg 1955; Mock and Kroon 2002; Palmucci et al. 2011). Although we found no changes in the abundance of proteins associated with this pathway and there were few changes in transcript levels (Mock et al. 2008), these studies provide an alternative hypothesis to explain responses to nitrogen starvation seen here. Indeed the protein and transcript data discussed here were collected in the early stages of nitrogen starvation and it is possible that fatty acid biosynthesis increases at a later stage in the response. The changes in protein abundance observed do suggest increased synthesis of acetyl CoA, which is a precursor for fatty acid biosynthesis.

But why break down carbohydrates while building fatty acid stores? Palmucci et al (2011) have shown that the diatoms *P. tricornutum* and *Thalassiosira weissflogii* reduce carbohydrate stores whilst

increasing levels of fatty acids under nitrogen starvation. They propose that fatty acids are more energy and reductant demanding than carbohydrates and that moving between these carbon stores increases the intracellular sink for these components. No change in either carbon store was found in *T. pseudonana*, but also no change in protein content (Palmucci et al. 2011). This suggests that nitrogen levels were not low enough to instigate a response to nitrogen starvation, and given a more severe starvation treatment, as used here, changes in carbon storage might occur.

If acetyl CoA is directed into fatty acid biosynthesis, how can the increase TCA enzymes be explained? It should be noted that most enzymes of the TCA cycle are not unidirectional and, under certain circumstances, can catalyse the reverse reaction. In their review Sweetlove et al (2010) propose that the flux of the TCA cycle is highly adaptable and is likely to reflect the physiological and metabolic demands of the cell. They discuss that in higher plants the 'conventional' cyclic flux of TCA, which produces reducing equivalents for ATP synthesis, is thought only to be active in the dark. In illuminated leaves of *Spinacia oleracea* the TCA cycle forms two branches, converting acetyl CoA to 2-oxoglutarate, for nitrogen assimilation, and oxaloacetate for aspartate biosynthesis (Hanning and Heldt 1993). Furthermore in *Brassica napus* seeds cultured with the amino acids alanine and glutamine as a nitrogen source, the carbon skeletons produced by their catabolism enter the TCA cycle and this directs the carbon in both the forward and, to a lesser extent, the reverse reactions to form citrate, which is then converted to acetyl CoA and used in fatty acid elongation (Schwender et al. 2006; Junker et al. 2007). The suggested catabolism of amino acids in *T. pseudonana* under nitrogen starvation would yield various TCA intermediates that could feed into the TCA cycle in this way (fig. 6) and be directed to fatty acid biosynthesis.

Concluding Remarks

Changes in the abundance of proteins identified in the current study, especially the increase in glycolytic and TCA cycle enzymes, suggest that the central carbon metabolism response of *T. pseudonana* to nitrogen starvation might differ considerably from that seen in other eukaryotic photoautotrophs studied to date. These pathways could be involved in providing carbon skeletons, for nitrogen reassimilation, or in the diversion of excess carbon into fatty acid biosynthesis. It is possible that both processes might have a place, with the TCA cycle acting as a hub, balancing the demand for specific carbon skeletons with the input of excess carbon from catabolic process in the cell. The similarity between the TCA cycle responses of *T. pseudonana* and the cyanobacteria *P. marinus*, both of which possess a urea cycle, suggests that the presence of this pathway might be closely related to the response of the TCA cycle seen here. The releationship between central carbon metabolism and the catabolic processes of the cell could play an important role in the success of diatoms in the ocean,

where nitrogen availability is highly dynamic. Given the potential for manipulation of nitrogen and carbon metabolism these findings also have relevance for algal and plant biofuels and crop nutrition research.

Materials and Methods

Culturing

Axenic cultures of *Thalassiosira pseudonana* (CCMP 1335) were grown in batch culture in ESAW (enriched seawater, artificial water) medium (Harrison and Berges 2005) at 15 ^{o}C, with a 14:10 light:dark cycle, at 115 µmol photons m^{-2} s^{-1} based on an immersed measurement with a Scalar PAR Irradiance Sensor QSL 2101 (Biospherical Instruments Inc., San Diego, USA). Cultures were regularly checked for bacterial contamination by 4',6-diamidino-2-phenylindoledihydrochloride (DAPI) staining (Porter and Feig 1980). Cell number and volume were measured with a Beckman Coulter Multisizer 3 Analyser (Beckman Coulter Ltd, High Wycombe, UK) and variable to maximum fluorescence ratio (F_v/F_m) with a Walz Phyto-Pam phytoplankton analyser (Heinz Walz GmbH, Effeltrich, Germany). Preliminary tests showed that when *T. pseudonana* cultures with an initial concentration of 550 µM nitrate were still in logarithmic growth cultures started with 30 µM nitrate were yield-limited at ca. $1x10^6$ cell ml^{-1}. Hence, triplicate cultures were started with initial concentrations of 550 µM nitrate (standard ESAW) or 30 µM nitrate. Samples were taken as low nitrate cultures reached the onset of nitrogen starvation (around $1x10^6$ cell ml^{-1}), with 250 ml filtered onto a 1.0 µm pore, 47 mm diameter nucleopore membrane (Whatman Plc, Maidstone, UK) at a pressure of 40 Kpa. Filters were immediately snap frozen in liquid nitrogen and stored at -80 ^{o}C.

Amino Acid Measurements

Cells were washed from the filter with 410 µl of methanol:buffer (3.5:0.6 v/v; buffer: 20 mM HEPES, pH 7.0, 5 mM EDTA, 10 mM NaF) and 150 µl chloroform was added. Samples were shaken at 4 ^{o}C for 30 min and 300 µl water was added, before shaking for a further 30 min at 37 ^{o}C. Samples were then centrifuged for 15 min at 11100 g at room temperature and the upper aqueous phase was taken. The lower chloroform phase was re-extracted with 300 µl water. Samples were dried in a speed vac at 37 ^{o}C and resuspended in 500 µl water. Of this, 15 µl was derivatised according to the AccQ Tag chemistry package (Waters Ltd, Elstree, UK) and 10 µl of the final solution was injected into a Waters 2695 HPLC, fitted with an AccQ-Tag (3.9 x 150mm) column and a 474 fluorescence detector (Waters). The values were calculated as intercellular concentration using the cell number and cell volume data.

Nitrate Measurements

Twenty five mg aliquots of polyvinylpolypyrrolidone (PVPP) were incubated with 1 ml deionised water over night at 4 °C. Diatom cells were washed from the filter with 500 µl of deionised water and centrifuged at 1500 g at 4 °C for 5 min. The supernatant was removed and cells were resuspended in 500 µl of the PVPP water mix. They were then disrupted by sonication (three times for 10 sec at ca. 15 microns on ice with a Soniprep 150 probe; MSE, London, UK). The homogenised sample was returned to the water-PVPP mix. Samples were shaken at 4 °C for 1 hour and then heated at 95 °C for 15 min. Finally they were centrifuged at 11100 g for 15 min at 4 °C and 100 µl was injected into a Waters 2695 HPLC, fitted with an ION-Pack ion exchange column (Waters). The ions were resolved in an isocratic flow (0.8 ml^{-1} min^{-1}) of Li-gluconate buffer and detected with a conductivity detector (Waters) as described in (North et al. 2009). The values were calculated as intercellular concentration using the cell number and cell volume data.

Protein extraction

Proteins were extracted based on Contreras et al (2008). Cells were washed from the filter with 800 µl extraction buffer (1.5 % w/v polyvinyl pyrrolidone, 0.7 M sucrose, 0.1 M potassium chloride, 0.5 M Tris-HCl pH 7.5, 250 mM EDTA and 0.5 % 3-[(3-cholamidopropyl)dimethylammonio]-1-propanesulfonate (CHAPS)) and 8 µl protease inhibitor cocktail for plant and tissue extracts (Sigma-Aldrich Company Ltd, Dorset, UK) was added. Cells were disrupted by sonication (detail above), followed by the addition of 16 µl mercaptoethanol. An equal volume of Tris-HCL pH 8 saturated phenol was added and samples were shaken on ice for 20 minutes. Samples were then centrifuged at 6600 g and 4 ^{o}C for 30 minutes. The upper phenol phase was removed to a 15 ml glass tube and kept on ice, while the lower buffer layer was re-extracted with phenol. Protein was precipitated by addition of 7.5 ml ice cold 0.1 M ammonium acetate in methanol and 3 hours incubation at -20 ^{o}C, followed by 20 min centrifugation at 10000 g and 4 ^{o}C. The supernatant was removed and the pellet was resuspended in 2 ml ice cold 0.1 M ammonium acetate in methanol, and incubated for a further 20 minutes at -20 ^{o}C. The protein was collected by 5 min centrifugation at 6600 g and 4^{o}C. The pellet was rinsed 4 times in ice cold acetone and stored at -80^{o}C.

Two-dimensional gel electrophoresis and protein identification

For the first dimension, 100 µg protein (extracted as above and quantified with an Ettan 2-D Quant kit; GE Healthcare, Chalfont, UK) were mixed with immobilized pH gradient (IPG) rehydration buffer (7 M urea, 2 M thiourea, 2% CHAPS, 18 mM dithiothreitol (DTT), bromophenol blue (trace amount to give blue colour) and 2% pH 4-7 IPG buffer; final volume 450 µl) before loading onto

24 cm pH 4-7 Immobiline DryStrips (GE Healthcare). Following overnight rehydration, isoelectric focusing was performed for 44.7 kVh at 20 °C over 8 h 45 min using the IPGphor system (GE Healthcare). Prior to the second dimension the focussed strips were conditioned in 122 mM Tris-acetate equilibration buffer supplemented with 5 mg ml^{-1} SDS, 360 mg ml^{-1} urea and 300 mg ml^{-1} glycerol. To reduce and alkylate cysteine residues, the strips were sequentially treated with equilibration buffer containing 8 mg ml^{-1} DTT, and then equilibration buffer containing 25 mg ml^{-1} iodoacetamide (each treatment consisted of 9 ml of buffer, 30 min with gentle shaking). For the second dimension, 10% Duracryl gels (28 x 23 cm; 1 mm thick) were prepared for use in the Investigator 2nd Dimension Running System (Genomic Solutions, Huntington, UK); with cathode buffer (200 mM Tris base, 200 mM Tricine, 14 mM SDS,) and anode buffer (25 mM Tris/acetate buffer, pH 8·3). Electrophoresis was carried out using 20 W per gel. Proteins were stained with Sypro-Ruby (Invitrogen Ltd, Paisley, UK), according to the manufacturer's instructions, and gel images were captured with a Pharos FX+ Molecular Imager with Quantity One imaging software (Invitrogen). A 532 nm excitation laser was used with a 605 nm band pass emission filter and gels were scanned at 100 µm resolution to produce a 16 bit image. Gel images were compared using Progenesis SameSpots analysis software (v4.1; Nonlinear Dynamics Ltd, Newcastle Upon Tyne, UK) and protein spots with altered levels of expression under nitrogen limitation versus control conditions were excised from the gel using a ProPick excision robot (Genomic Solutions).

The protein was then manually in-gel trypsin digested by first washing in 100 µl 400 mM ammonium bicarbonate : 100% acetonitrile (1:1) for 20 min to equilibrate the gel to pH 8 and to remove the stain. This was repeated. Aqueous solutions were then removed by washing briefly with 100 µl acetonitrile. The gel was then washed again in 100 µl acetonitrile for 15 min to shrink the gel before air drying for 10 min. The protein was digested by the addition of 50 ng Trypsin in 5 µl 10 mM ammonium bicarbonate (Modified porcine trypsin, Promega, Madison, USA) and samples were incubated at 37 °C for 3 h. Samples were acidified by incubating with 5 µl 5% formic acid for 10 min, before flash freezing and storing at -80^{o}C.

Tryptic digests were analysed by peptide mass fingerprinting (Pappin et al. 1993). The acidified digests were spotted directly onto a pre-spotted anchor chip (PAC) target plate (Bruker UK Ltd, Coventry, UK) which is pre-coated with α-cyano-4-hydroxycinnamic acid matrix. Mass analysis was carried out on an Ultraflex MALDI-ToF/ToF mass spectrometer (Bruker UK). A 50 Hz nitrogen laser was used to desorb/ionise the matrix/analyte material, and ions were automatically detected in positive ion reflectron mode first with and then without the use of fuzzy logic programming. The

calibrated spectra were searched against a monthly updated copy of the SPtrEMBL database, using an in-house version (v2.2) of the MASCOT search tool (reference: http://www.matrixscience.com).

Supplemental Data

The following materials are available in the online version of this article.

Supplemental Figure 1. Growth and photosystem II efficiency (Fv/Fm) of nitrogen starved *T. pseudonana* cultures compared to nitrogen replete cultures.

Supplemental Table 1. Proteins that changed in abundance in nitrogen starved *T. pseudonana*, compared to nitrogen replete cultures.

Supplemental Table 2. Interspecies comparison of changes in transcript levels of genes involved in C-metabolism associated with nitrogen deprivation.

Acknowledgments

We thank Gareth Lee and Rob Utting (University of East Anglia) and Anna Koprivova (John Innes Centre) for their technical support and Lynn Olivier (Institute of Food Research) for advising on 2d-gel electrophoresis methods. We are also grateful to Mike Naldrett (John Innes Centre) for conducting mass spectrometry analysis and to Baldeep Kular (John Innes Centre) for measuring amino acid.

Literature Cited

Allen AE,Dupont CL,Obornik M,Horak A,Nunes-Nesi A,McCrow JP,Zheng H,Johnson DA,Hu HH,Fernie AR,Bowler C (2011) Evolution and metabolic significance of the urea cycle in photosynthetic diatoms. *Nature* **473**: 203-207.

Allen AE,Vardi A,Bowler C (2006) An ecological and evolutionary context for integrated nitrogen metabolism and related signaling pathways in marine diatoms. *Curr. Opin. Plant Biol.* **9**: 264-273.

Allen AE,Ward BB,Song BK (2005) Characterization of diatom (Bacillariophyceae) nitrate reductase genes and their detection in marine phytoplankton communities. *J. Phycol.* **41**: 95-104.

Andreae MO (1986) The ocean as a source of atmospheric sulphur compounds. In P Buat-Menard, eds, The role of air-sea exchange in geochemical cycling. Reidel, New York, pp 331-362

Armbrust EV,Berges JA,Bowler C,Green BR,Martinez D,Putnam NH,Zhou SG,Allen AE,Apt KE,Bechner M,Brzezinski MA,Chaal BK,Chiovitti A,Davis AK,Demarest MS,Detter JC,Glavina T,Goodstein D,Hadi MZ,Hellsten U,Hildebrand M,Jenkins BD,Jurka J,Kapitonov VV,Kroger N,Lau WWY,Lane TW,Larimer FW,Lippmeier JC,Lucas S,Medina M,Montsant A,Obornik M,Parker MS,Palenik B,Pazour GJ,Richardson PM,Rynearson TA,Saito MA,Schwartz DC,Thamatrakoln K,Valentin K,Vardi A,Wilkerson FP,Rokhsar DS (2004) The genome of the diatom *Thalassiosira pseudonana*: Ecology, evolution, and metabolism. *Science* **306**: 79-86.

Berges JA,Harrison PJ (1995) Nitrate reductase-activity quantitatively predicts the rate of nitrate incorporation under steady-state light limitation - A revised assay and characterization of the enzyme in 3 species of marine-phytoplankton. *Limnol. Oceanogr.* **40**: 82-93.

Bowler C,Allen AE,Badger JH,Grimwood J,Jabbari K,Kuo A,Maheswari U,Martens C,Maumus F,Otillar RP,Rayko E,Salamov A,Vandepoele K,Beszteri B,Gruber A,Heijde

M,Katinka M,Mock T,Valentin K,Verret F,Berges JA,Brownlee C,Cadoret JP,Chiovitti A,Choi CJ,Coesel S,De Martino A,Detter JC,Durkin C,Falciatore A,Fournet J,Haruta M,Huysman MJJ,Jenkins BD,Jiroutova K,Jorgensen RE,Joubert Y,Kaplan A,Kroger N,Kroth PG,La Roche J,Lindquist E,Lommer M,Martin-Jezequel V,Lopez PJ,Lucas S,Mangogna M,McGinnis K,Medlin LK,Montsant A,Oudot-Le Secq MP,Napoli C,Obornik M,Parker MS,Petit JL,Porcel BM,Poulsen N,Robison M,Rychlewski L,Rynearson TA,Schmutz J,Shapiro H,Siaut M,Stanley M,Sussman MR,Taylor AR,Vardi A,von Dassow P,Vyverman W,Willis A,Wyrwicz LS,Rokhsar DS,Weissenbach J,Armbrust EV,Green BR,Van De Peer Y,Grigoriev IV (2008) The *Phaeodactylum* genome reveals the evolutionary history of diatom genomes. *Nature* **456**: 239-244.

Bowler C,Vardi A,Allen AE (2010) Oceanographic and biogeochemical insights from diatom genomes. *Annual Review of Marine Science* **2**: 333-365.

Brown KL,Twing KI,Robertson DL (2009) Unraveling the regulation of nitrogen assimilation in the marine diatom *Thalassiosira pseudonana* (Bacillariophyceae): Diurnal variations in transcript levels for five genes involved in nitrogen assimilation. *J. Phycol.* **45**: 413-426.

Clayton JR,Ahmed SI (1986) Detection of glutamate synthase (GOGAT) activity in phytoplankton - Evaluation of cofactors and assay optimization. *Mar. Ecol. Prog. Ser.* **32**: 115-122.

Collyer DM,Fogg GE (1955) Studies on fat accumulation by algae. *J. Exp. Bot.* **6**: 256-275.

Contreras L,Ritter A,Dennett G,Boehmwald F,Guitton N,Pineau C,Moenne A,Potin P,Correa JA (2008) Two-dimensional gel electrophoresis analysis of brown algal protein extracts. *J. Phycol.* **44**: 1315-1321.

Diaz C,Purdy S,Christ A,Morot-Gaudry JF,Wingler A,Masclaux-Daubresse CL (2005) Characterization of markers to determine the extent and variability of leaf senescence in *Arabidopsis*. A metabolic profiling approach. *Plant Physiol.* **138**: 898-908.

Dickson DMJ,Kirst GO (1987) Osmotic adjustment in marine eukaryotic algae - The role of inorganic-ions, quaternary ammonium, tertiary sulfonium and carbohydrate solutes 1. Diatoms and a Rhodophyte. *New Phytol.* **106**: 645-655.

Dortch Q,Ahmed SI,Packard T (1979) Nitrate reductase and glutamate dehydrogenase activities in *Skeletonema costatum* as measures of nitrogen assimilation rates *J. Plankton Res.* **1**: 169-186.

Estrada M,Blasco D (1979) 2 phases of the phytoplankton community in the Baja California upwelling. *Limnol. Oceanogr.* **24**: 1065-1080.

Falkowski PG (1997) Evolution of the nitrogen cycle and its influence on the biological sequestration of CO_2 in the ocean. *Nature* **387**: 272-275.

Falkowski PG,Katz ME,Knoll AH,Quigg A,Raven JA,Schofield O,Taylor FJR (2004) The evolution of modern eukaryotic phytoplankton. *Science* **305**: 354-360.

Field CB,Behrenfeld MJ,Randerson JT,Falkowski P (1998) Primary production of the biosphere: Integrating terrestrial and oceanic components. *Science* **281**: 237-240.

Gao Y,Smith GJ,Alberte RS (1993) Nitrate reductase from the marine diatom *Skeletonema costatum* - Biochemical and immunological characterization. *Plant Physiol.* **103**: 1437-1445.

Hanning I,Heldt HW (1993) On the function of mitochondrial metabolism during photosynthesis in Spinach (*Spinacia-oleracea L*) leaves - partitioning between respiration and export of redox equivalents and precursors for nitrate assimilation products. *Plant Physiol.* **103**: 1147-1154.

Harrison PJ,Berges JA (2005) Marine culture medium. In RA Andersen, eds, Algal Culturing Techniques. Academic Press, San Diego, pp 21-33.

Junker BH,Lonien J,Heady LE,Rogers A,Schwender J (2007) Parallel determination of enzyme activities and *in vivo* fluxes in *Brassica napus* embryos grown on organic or inorganic nitrogen source. *Phytochemistry* **68**: 2232-2242.

Keller MD,Kiene RP,Matrai PA,Bellows WK (1999) Production of glycine betaine and dimethylsulfoniopropionate in marine phytoplankton. II. N-limited chemostat cultures. *Mar. Biol.* **135**: 249-257.

Kroth PG,Chiovitti A,Gruber A,Martin-Jezequel V,Mock T,Parker MS,Stanley MS,Kaplan A,Caron L,Weber T,Maheswari U,Armbrust EV,Bowler C (2008) A Model for

Carbohydrate Metabolism in the Diatom *Phaeodactylum tricornutum* Deduced from Comparative Whole Genome Analysis. *Plos One* **3**.

Logan BA,Demmig-Adams B,Rosenstiel TH,Adams WW (1999) Effect of nitrogen limitation on foliar antioxidants in relationship to other metabolic characteristics. *Planta* **209**: 213-220.

Mann KH (1993) Physical oceanography, food chains, and fish stocks - A review. *ICES J. Mar. Sci.* **50**: 105-119.

Miller R,Wu GX,Deshpande RR,Vieler A,Gartner K,Li XB,Moellering ER,Zauner S,Cornish AJ,Liu BS,Bullard B,Sears BB,Kuo MH,Hegg EL,Shachar-Hill Y,Shiu SH,Benning C (2010) Changes in transcript abundance in *Chlamydomonas reinhardtii* following nitrogen deprivation predict diversion of metabolism. *Plant Physiol.* **154**: 1737-1752.

Milligan AJ,Harrison PJ (2000) Effects of non-steady-state iron limitation on nitrogen assimilatory enzymes in the marine diatom *Thalassiosira weissflogii* (Bacillariophyceae). *J. Phycol.* **36**: 78-86.

Mock T,Kroon BMA (2002) Photosynthetic energy conversion under extreme conditions - I: important role of lipids as structural modulators and energy sink under N-limited growth in Antarctic sea ice diatoms. *Phytochemistry* **61**: 41-51.

Mock T,Samanta MP,Iverson V,Berthiaume C,Robison M,Holtermann K,Durkin C,BonDurant SS,Richmond K,Rodesch M,Kallas T,Huttlin EL,Cerrina F,Sussmann MR,Armbrust EV (2008) Whole-genome expression profiling of the marine diatom *Thalassiosira pseudonana* identifies genes involved in silicon bioprocesses. *PNAS* **105**: 1579-1584.

Moellering ER,Benning C (2010) RNA interference silencing of a major lipid droplet protein affects lipid droplet size in *Chlamydomonas reinhardtii*. *Eukaryot. Cell* **9**: 97-106.

Nelson DM,Treguer P,Brzezinski MA,Leynaert A,Queguiner B (1995) Production and dissolution of biogenic silica in the ocean - Revised global estimates, comparison with regional data and relationship to biogenic sedimentation. *Global Biogeochem. Cy.* **9**: 359-372.

North KA,Ehlting B,Koprivova A,Rennenberg H,Kopriva S (2009) Natural variation in Arabidopsis adaptation to growth at low nitrogen conditions. *Plant Physiol. Biochem.* **47**: 912-918.

Nunn BL,Aker JR,Shaffer SA,Tsai YH,Strzepek RF,Boyd PW,Freeman TL,Brittnacher M,Malmstrom L,Goodlett DR (2009) Deciphering diatom biochemical pathways via whole-cell proteomics. *Aquat. Microb. Ecol.* **55**: 241-253.

Palmucci M,Ratti S,Giordano M (2011) Ecological and evolutionary implications of carbon allocation in marine phytoplankton as a function of nitrogen availability: A fourier transform infrared spectroscopy approach. *J. Phycol.* **47**: 313-323.

Pappin DJC,Hojrup P,Bleasby AJ (1993) Rapid identification of proteins by peptide-mass fingerprinting. *Curr. Biol.* **3**: 327-332.

Parker MS,Armbrust EV (2005) Synergistic effects of light, temperature, and nitrogen source on transcription of genes for carbon and nitrogen metabolism in the centric diatom *Thalassiosira pseudonana* (Bacillariophyceae). *J. Phycol.* **41**: 1142-1153.

Peng MS,Bi YM,Zhu T,Rothstein SJ (2007) Genome-wide analysis of *Arabidopsis* responsive transcriptome to nitrogen limitation and its regulation by the ubiquitin ligase gene *NLA*. *Plant Mol. Biol.* **65**: 775-797.

Porter KG,Feig YS (1980) The use of DAPI for identifying and counting aquatic microflora. *Limnol. Oceanogr.* **25**: 943-948.

Poulsen N,Kroger N (2005) A new molecular tool for transgenic diatoms - Control of mRNA and protein biosynthesis by an inducible promoter-terminator cassette. *FEBS J.* **272**: 3413-3423.

Robertson DL,Alberte RS (1996) Isolation and characterization of glutamine synthetase from the marine diatom *Skeletonema costatum*. *Plant Physiol.* **111**: 1169-1175.

Robertson DL,Smith GJ,Alberte RS (1999) Characterization of a cDNA encoding glutamine synthetase from the marine diatom *Skeletonema costatum* (Bacillariophyceae). *J. Phycol.* **35**: 786-797.

Robertson DL,Tartar A (2006) Evolution of glutamine synthetase in heterokonts: Evidence for endosymbiotic gene transfer and the early evolution of photosynthesis. *Mol. Biol. Evol.* **23**: 1048-1055.

Sauer J,Dirmeier U,Forchhammer K (2000) The *Synechococcus* strain PCC 7942 glnN product (glutamine synthetase III) helps recovery from prolonged nitrogen chlorosis. *J. Bacteriol.* **182**: 5615-5619.

Schwender J,Shachar-Hill Y,Ohlrogge JB (2006) Mitochondrial metabolism in developing embryos of *Brassica napus*. *J. Biol. Chem.* **281**: 34040-34047.

Siaut M,Heijde M,Mangogna M,Montsant A,Coesel S,Allen A,Manfredonia A,Falciatore A,Bowler C (2007) Molecular toolbox for studying diatom biology in *Phaeodactylum tricornutum*. *Gene* **406**: 23-35.

Stefels J (2000) Physiological aspects of the production and conversion of DMSP in marine algae and higher plants. *J. Sea Res.* **43**: 183-197.

Sunda W,Kieber DJ,Kiene RP,Huntsman S (2002) An antioxidant function for DMSP and DMS in marine algae. *Nature* **418**: 317-320.

Sweetlove LJ,Beard KFM,Nunes-Nesi A,Fernie AR,Ratcliffe RG (2010) Not just a circle: Flux modes in the plant TCA cycle. *Trends Plant Sci.* **15**: 462-470.

Takabayashi M,Wilkerson FP,Robertson D (2005) Response of glutamine synthetase gene transcription and enzyme activity to external nitrogen sources in the diatom *Skeletonema costatum* (Bacillariophyceae). *J. Phycol.* **41**: 84-94.

Tanaka R,Oster U,Kruse E,Rudiger W,Grimm B (1999) Reduced activity of geranylgeranyl reductase leads to loss of chlorophyll and tocopherol and to partially geranylgeranylated chlorophyll in transgenic tobacco plants expressing antisense RNA for geranylgeranyl reductase. *Plant Physiol.* **120**: 695-704.

Tolonen AC,Aach J,Lindell D,Johnson ZI,Rector T,Steen R,Church GM,Chisholm SW (2006) Global gene expression of *Prochlorococcus* ecotypes in response to changes in nitrogen availability. *Mol. Syst. Biol.* **2**: 53.

Vergara JJ,Berges JA,Falkowski PG (1998) Diel periodicity of nitrate reductase activity and protein levels in the marine diatom *Thalassiosira weissflogii* (Bacillariophyceae). *J. Phycol.* **34**: 952-961.

Voellmy R,Leisinger T (1975) Dual role for N2-acetylornithine 5-aminotransferase from *Pseudomonas aeruginosa* in arginine biosynthesis and arginine catabolism. *J. Bacteriol.* **122**: 799-809.

Wang ZT,Ullrich N,Joo S,Waffenschmidt S,Goodenough U (2009) Algal lipid bodies: Stress induction, purification, and biochemical characterization in wild-type and starchless *Chlamydomonas reinhardtii*. *Eukaryot. Cell* **8**: 1856-1868.

Wingler A,Purdy S,MacLean JA,Pourtau N (2006) The role of sugars in integrating environmental signals during the regulation of leaf senescence. *J. Exp. Bot.* **57**: 391-399.

Zadykowicz E,Robertson D (2005). Phylogenetic relationships amongst glutamate synthase enzymes. 44th Northeast Algal Symposium, Rockland, Maine, pp 41.

Zehr JP,Falkowski PG (1988) Pathway of ammonium assimilation in a marine diatom determined with the radiotracer ^{13}N. *J. Phycol.* **24**: 588-591.

Figure Legends

Figure 1. Intracellular concentration of free nitrate, amino acids, and protein in nitrogen replete (550 µM nitrate) and nitrogen starved (30 µM nitrate*) T. pseudonana* cultures at the onset of nitrogen starvation. Results are shown as means of 3 biological replicates ± standard deviation.

Figure 2. Effect of nitrogen starvation on the proteome of *T. pseudonana*. Soluble proteins were isolated from *T. pseudonana* cultures grown in nitrogen replete (550 µM nitrate) and nitrogen starved (30 µM nitrate) conditions and resolved by 2-D electrophoresis. Gels of three biological replicates were used for quantitative analysis and for this illustration representative gels from each treatment were overlaid. Equal protein abundance is represented by black spots, blue spots represent proteins more abundant in N starved cells while orange represents proteins more abundant in N replete cells. Examples of proteins of interest (A-L) are expanded. A. Citrate synthase (ProtID 11411). B. Aconitase hydratase (ProtID 268965). C. Isocitrate dehydrogenase (ProtID 21640). D. Pyruvate dehydrogenase (ProtID 8778). E. Pyruvate dehydrogenase (ProtID 268374). F. NADPH-dependent nitrite reductase (ProtID 26941). G. Branched-chain aminotransferase (ProtID 260934). H. Phosphoenolpyruvate carboxylase (ProtID 268546). I. Nitrate reductase (ProtID 25299). J. Ferredoxin-dependent nitrite reductase (ProtID 262125). K. NAD(P)H-dependent glutamate synthase (ProtID 269160). L. Type III glutamine synthetase (ProtID 270138). Where multiple spots are circled the same protein occurs as more than one spot on the gel most likely due to pI differences caused by post-translational modifications.

Figure 3. Categories of genes and proteins altered in expression between nitrogen starved and replete *T. pseudonana* cells. Categorisation is based on KEGG, some categories were split to subcategories to illustrate points of specific interest, whereas categories that were under represented were merged with related groups. A. Proteins increased in abundance. Of 42 proteins increasing in abundance 32 could be assigned a function, of which 4 are not represented by this categorisation. B. Proteins decreased in abundance. From 23 proteins decreased in abundance, 18 could be assigned a function. C. Transcripts more highly expressed in N starved cells (Mock et al 2008). Of 305 transcripts that increased in abundance 101 could be assigned a function, of which 23 are not represented. D. Transcripts decreased in expression. 362 transcripts decreased in abundance and 167 were assigned a function, of which 27 are not represented.

Figure 4. Representation of the changes in the abundance of proteins associated with nitrogen assimilation in *T. pseudonana*, brought on by the onset of nitrogen starvation. Increases are shown by bold arrows and decreases by dashed arrows.

Figure 5. Intracellular concentration of individual amino acids in nitrogen replete (550 µM nitrate) and nitrogen starved (30 µM nitrate) *T. pseudonana* cells. A. The most abundant and B. the least

abundant amino acids were determined by HPLC. Results are shown as means of 3 biological replicates ± standard deviation.

Figure 6. Representation of the changes in the abundance of proteins associated with carbon metabolism in *T. pseudonana* at the onset of nitrogen starvation. Increases are shown by bold arrows and no decreases were seen. Boxes show where carbon skeletons from amino acid degradation feed into the pathway.

Figure 7. A comparison of changes in transcript levels associated with nitrogen deprivation in A. *T. pseudonana*, grown under conditions comparable to the current study (Mock et al 2008). B. *C. reinhardtii*, 48 h after the transfer of cells from 10 mM ammonium to nitrogen free medium. (Miller et al 2010). C. *A. thaliana*, at the onset of nitrogen limitation in plants grown with 3 mM nitrate (Peng et al 2007). D. *P. marinus* (MED4), 24 h after transfer from 800 µM ammonium into nitrogen free medium (Tolonen et al. 2006). Genes for each enzyme were identified using the genome databases for each species (*T. pseudonana*: http://genome.jgi-psf.org/Thaps3/Thaps3.home.html; *C. reinhardtii*: http://genome.jgi-psf.org/Chlre4/Chlre4.home.html; *A. thaliana*: www.arabidopsis.org; *P. marinus*: http://img.jgi.doe.gov/cgi-bin/w/main.cgi) and these were searched against the expression profiles presented in the four publications above to identify the degree of change in transcript level. Each box represents an isoform and multiple rows show that there is more than one enzyme responsible for a specific step. See Supplemental Table 2 for EC numbers and accession numbers. Red shows that transcript increased, green shows a decrease and blue shows stable transcript level.

Table 1. Proteins involved in nitrogen, protein and amino acid metabolism with a greater than 1.5 fold change ($P<0.05$) in *T. pseudonana* at the onset of nitrogen starvation, compared to nitrogen replete cultures. Values are based on three biological replicates. Protein name is based on UniProtKB unless otherwise stated and Protein IDs are from the Joint Genome Institute *T. pseudonana* genome version 3 (http://genome.jgi-psf.org/Thaps3/Thaps3.home.html). Multiple values are given for any protein represented by more than one spot on the 2-D gels. Microarray Log2 gives the fold change in transcript level of the corresponding gene under comparable nitrogen starved conditions as described by Mock et al (2008).

Protein ID	Protein Name	Fold Change	p	Microarray Log2
Nitrogen Assimilation				
25299	Nitrate reductase[mbc]	-10.72 -9.69 -8.81	0.00001 0.00002 0.00005	ND
26941	NADPH nitrite reductase	-3.01	0.00012	ND
262125	Nitrite reductase-ferredoxin dependent	-3.67 -3.04 -1.95 -1.71	0.00010 0.00001 0.00095 0.00108	ND
269160	NAD(P)H Glutamate Synthase	2.93 1.80 1.74	0.00124 0.00310 0.00031	1.71
270138	Glutamine synthetase type III [mbc]	1.63 1.61 1.51	0.00090 0.00233 0.00063	ND
Amino Acid Metabolism				
260934	Branched-chain-amino-acid aminotransferase	6.39	0.00008	3.08
28544	Dihydrodipicolinate reductase[mbc]	1.62	0.00211	1.48
25130	D-isomer specific 2-hydroxyacid dehydrogenase[mbc]	-1.73	0.00214	ND
23175	Acetolactate synthase[mb]	-1.97	0.00478	ND
22208	Class V aminotransferase[mbc]	1.86	0.00203	- 2.56
bd1806[l]	DegT/DnrJ/EryC1/StrS aminotransferase[mbc]	1.67 -2.26	0.00156 0.00001	ND
Protein Metabolism				
21235	S1 ribosomal protein[mc]	-2.01	0.00054	ND
15259	S1 ribosomal protein	-3.36 -2.93	0.00002 0.00137	ND
31912	Peptidyl-prolyl cis-trans isomerase	1.65	0.00463	ND
13254	RNA helicase	-2.28	0.00115	ND
269148	Translation factor tu domain 2	-1.94 -1.66	0.00266 0.00500	ND
15093	Serine carboxypeptidase	2.03	0.00093	1.1
Urea Cycle and Arginine Metabolism				
270136	N-acetylornithine aminotransferase	2.37	0.00006	1.77
21290	N-acetyl-gamma-glutamyl-phosphate reductase	1.74	0.00048	ND
30193	Urease	1.62[z]	0.00271	ND

[m] Manual Annotation. [b] Supported by BlastP ($E<1x10^{-50}$). [c] Supported by conserved domains identified through Pfam. [l] Location: bd_10x65:12123-13902. [z] Combined with another protein, making fold change imprecise. ND not detected.

Table 2. Proteins involved in photosynthesis and carbon metabolism, that had a greater than 1.5 fold change ($P<0.05$) in *T. pseudonana* at the onset of nitrogen starvation, compared to nitrogen replete cultures. Values are based on three biological replicates Protein name is based on UniProtKB unless otherwise stated and Protein IDs are from the Joint Genome Institute *T. pseudonana* genome version 3 (http://genome.jgi-psf.org/Thaps3/Thaps3.home.html). Multiple values are given for any protein represented by more than one spot on the 2-D gels. Microarray Log2 gives the fold change in transcript level of the corresponding gene under comparable nitrogen starved conditions as described by Mock et al (2008).

Protein ID	Protein Name	Fold Change	p	Microarray Log2
Chlorophyll Biosynthesis				
258111	Glutamate-1-semialdehyde aminotransferase[mb]	-1.61	0.00469	ND
270378	Magnesium-protoporphyrin IX methyltransferase[mbc]	-2.69	0.00013	ND
270312	1-deoxy-D-xylulose-5-phosphate synthase[mbc]	-2.14	0.00043	ND
29228	1-hydroxy-2-methyl-2-(E)-butenyl-4-diphosphate synthase[mbc]	-1.98	0.00050	ND
10234	Geranyl-geranyl reductase[mb]	-2.33 -1.92	0.00059 0.00248	-3.98
Antioxidant				
40713	Superoxide dismutase	1.89	0.00307	ND
38428	Mitochondrial alternative oxidase	2.24	0.00106	ND
Glycolysis and Gluconeogenesis				
40391	Enolase	1.52	0.00249	1.83
27850	Phosphoglycerate mutase	1.83	0.00241	2.99
270288	Fructose-bisphosphate aldolase[mbc]	1.83 1.80 1.72	0.00056 0.00356 0.00188	ND
31636	Aldose-1-epimerase	-2.37	0.00106	-1.57
26678	Transketolase	1.63	0.00254	ND
21175	Transketolase	-1.55	0.00450	-5.62
22301	Phosphomannomutase	1.68	0.00040	ND
Pyruvate Metabolism				
268546	Phosphoenolpyruvate carboxylase	2.53 2.52 1.79 1.62[z]	0.00104 0.00013 0.00206 0.00271	ND
268374	Pyruvate dehydrogenase	2.27 1.78	0.00218 0.00077	2.49
8778	Pyruvate dehydrogenase	2.09 1.76	0.00013 0.00004	2.99
268280	Dihydrolipoamide s-acetyltransferase	1.95	0.00064	ND
TCA Cycle				
11411	Citrate synthase	2.24 1.76	0.00429 0.00037	2.09
268965	Aconitase hydratase 2	1.70 1.62	0.00069 0.00089	1.96
1456	Isocitrate Dehydrogenase	1.62	0.00354	-1.38
21640	Isocitrate dehydrogenase[mbc]	1.66 1.53	0.00015 0.00418	1.73
42475	Succinate dehydrogenase flavoprotein subunit	1.89 1.79	0.00417 0.00196	ND
22464	Fumarate hydratase	2.49	0.00014	ND

[m] Manual Annotation. [b] Supported by BlastP ($E<1x10^{-50}$). [c] Supported by conserved domains identified through Pfam. [z] Combined with another protein, making fold change imprecise. ND not detected.

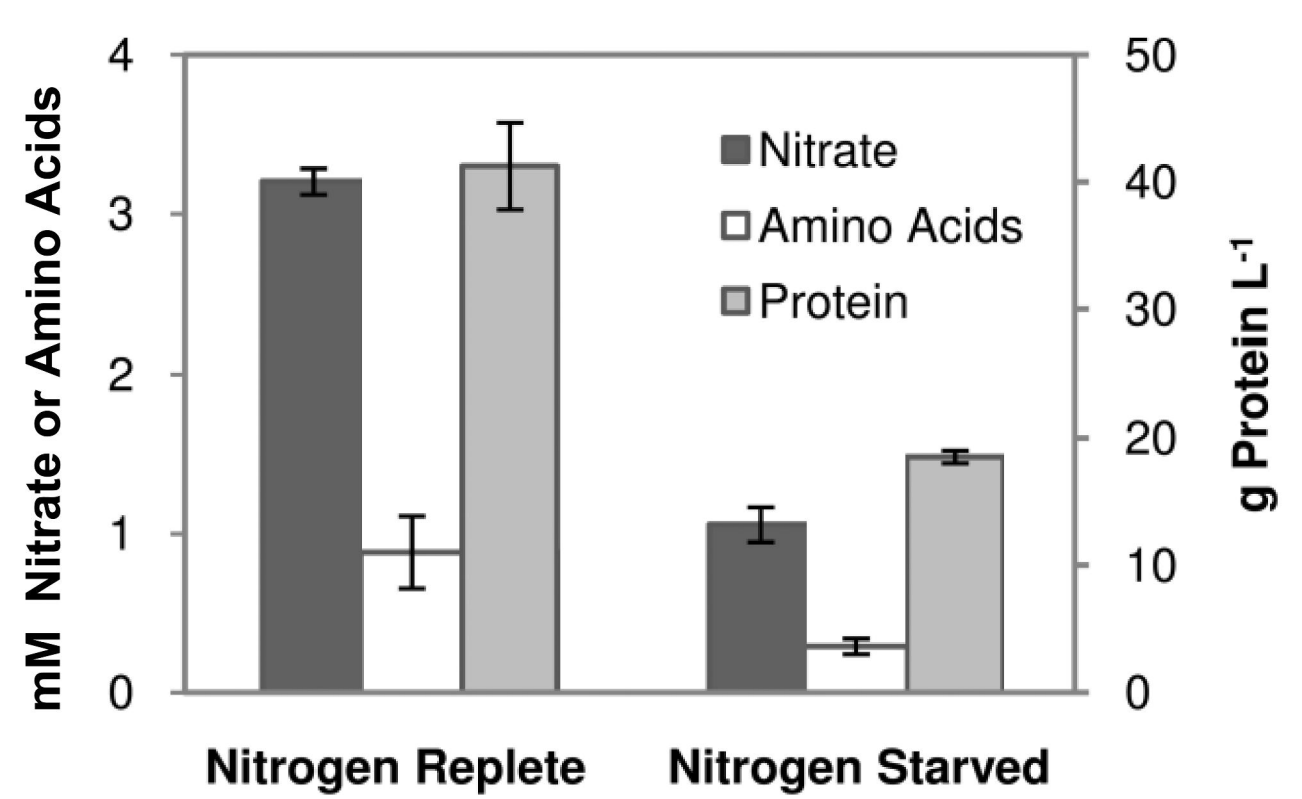

Figure 1. Intracellular concentration of free nitrate, amino acids, and protein in nitrogen replete (550 μM nitrate) and nitrogen starved (30 μM nitrate) T. pseudonana cultures at the onset of nitrogen starvation. Results are shown as means of 3 biological replicates ± standard deviation.

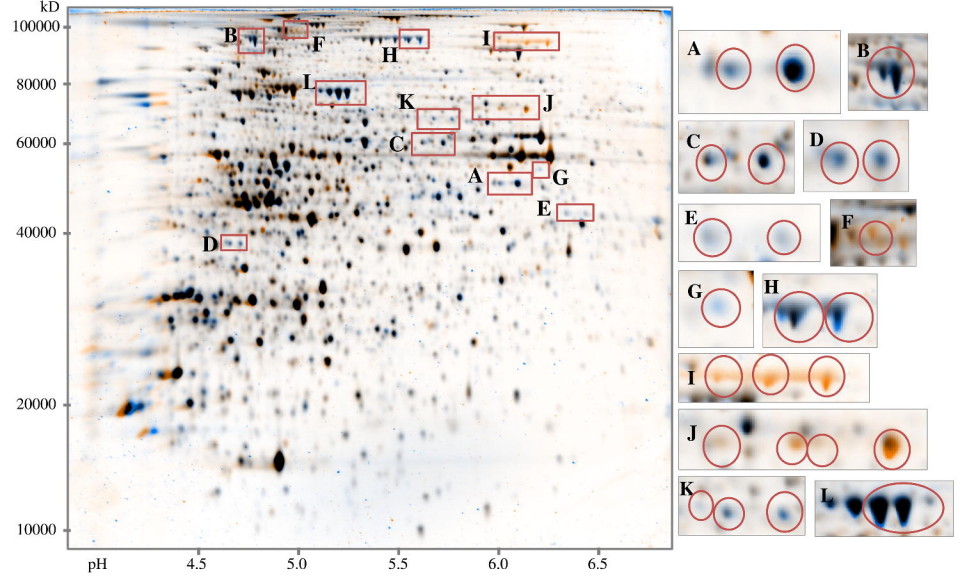

Figure 2. Effect of nitrogen starvation on the proteome of *T. pseudonana*. Soluble proteins were isolated from *T. pseudonana* cultures grown in nitrogen replete (550 µM nitrate) and nitrogen starved (30 µM nitrate) conditions and resolved by 2-D electrophoresis. Gels of three biological replicates were used for quantitative analysis and for this illustration representative gels from each treatment were overlaid. Equal protein abundance is represented by black spots, blue spots represent proteins more abundant in N starved cells while orange represents proteins more abundant in N replete cells. Examples of proteins of interest (A-L) are expanded. A. Citrate synthase (ProtID 11411). B. Aconitase hydratase (ProtID 268965). C. Isocitrate dehydrogenase (ProtID 21640). D. Pyruvate dehydrogenase (ProtID 8778). E. Pyruvate dehydrogenase (ProtID 268374). F. NADPH-dependent nitrite reductase (ProtID 26941). G. Branched-chain aminotransferase (ProtID 260934). H. Phosphoenolpyruvate carboxylase (ProtID 268546). I. Nitrate reductase (ProtID 25299). J. Ferredoxin-dependent nitrite reductase (ProtID 262125). K. NAD(P)H-dependent glutamate synthase (ProtID 269160). L. Type III glutamine synthetase (ProtID 270138). Where multiple spots are circled the same protein occurs as more than one spot on the gel most likely due to pI differences caused by post-translational modifications.

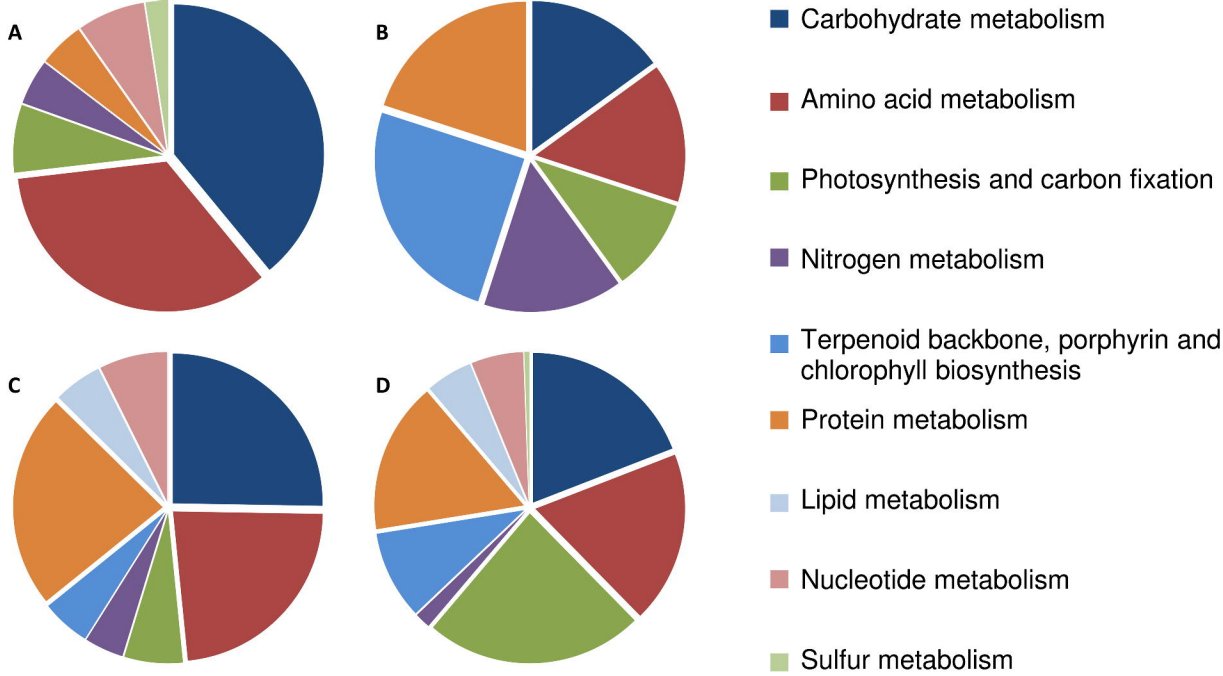

Figure 3. Categories of genes and proteins altered in expression between nitrogen starved and replete *T. pseudonana* cells. Categorisation is based on KEGG, some categories were split to subcategories to illustrate points of specific interest, whereas categories that were under represented were merged with related groups. A. Proteins increased in abundance. Of 42 proteins increasing in abundance 32 could be assigned a function, of which 4 are not represented by this categorisation. B. Proteins decreased in abundance. From 23 proteins decreased in abundance, 18 could be assigned a function. C. Transcripts more highly expressed in N starved cells (Mock et al 2008). Of 305 transcripts that increased in abundance 101 could be assigned a function, of which 23 are not represented. D. Transcripts decreased in expression. 362 transcripts decreased in abundance and 167 were assigned a function, of which 27 are not represented.

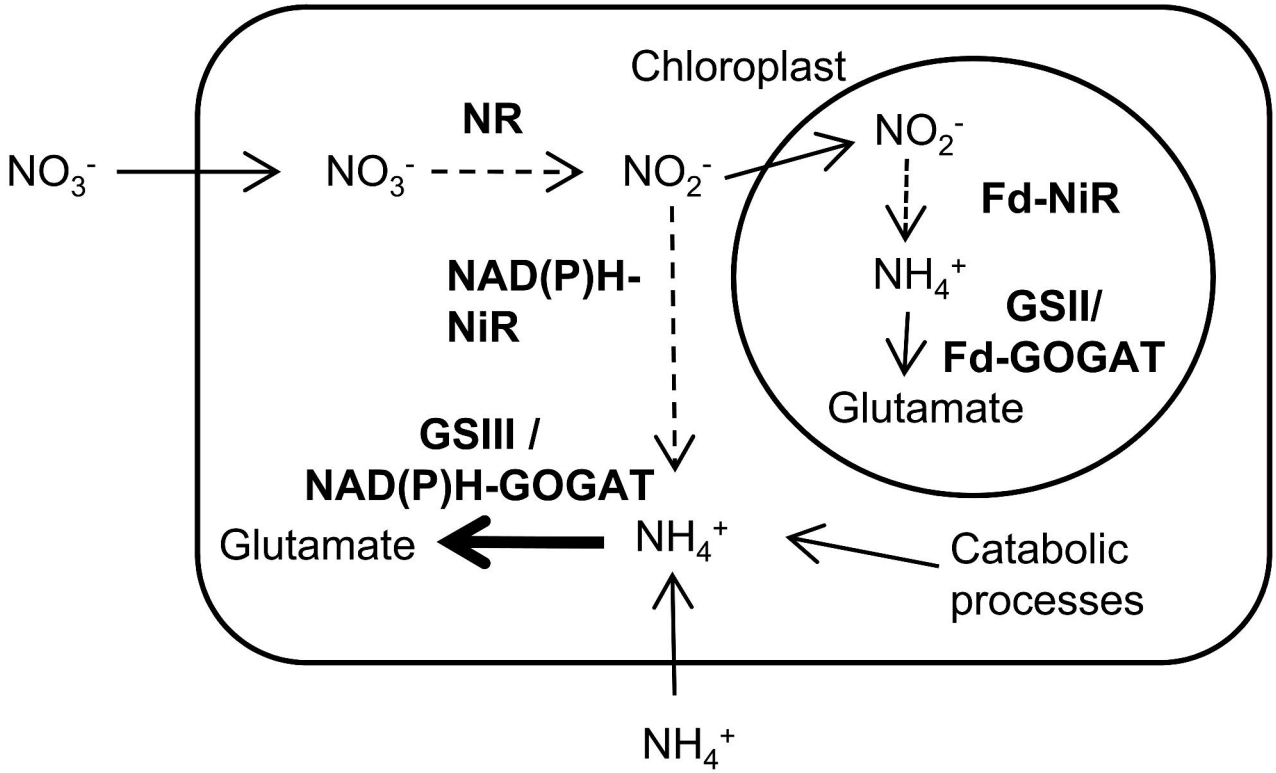

Figure 4. Representation of the changes in the abundance of proteins associated with nitrogen assimilation in *T. pseudonana*, brought on by the onset of nitrogen starvation. Increases are shown by bold arrows and decreases by dashed arrows.

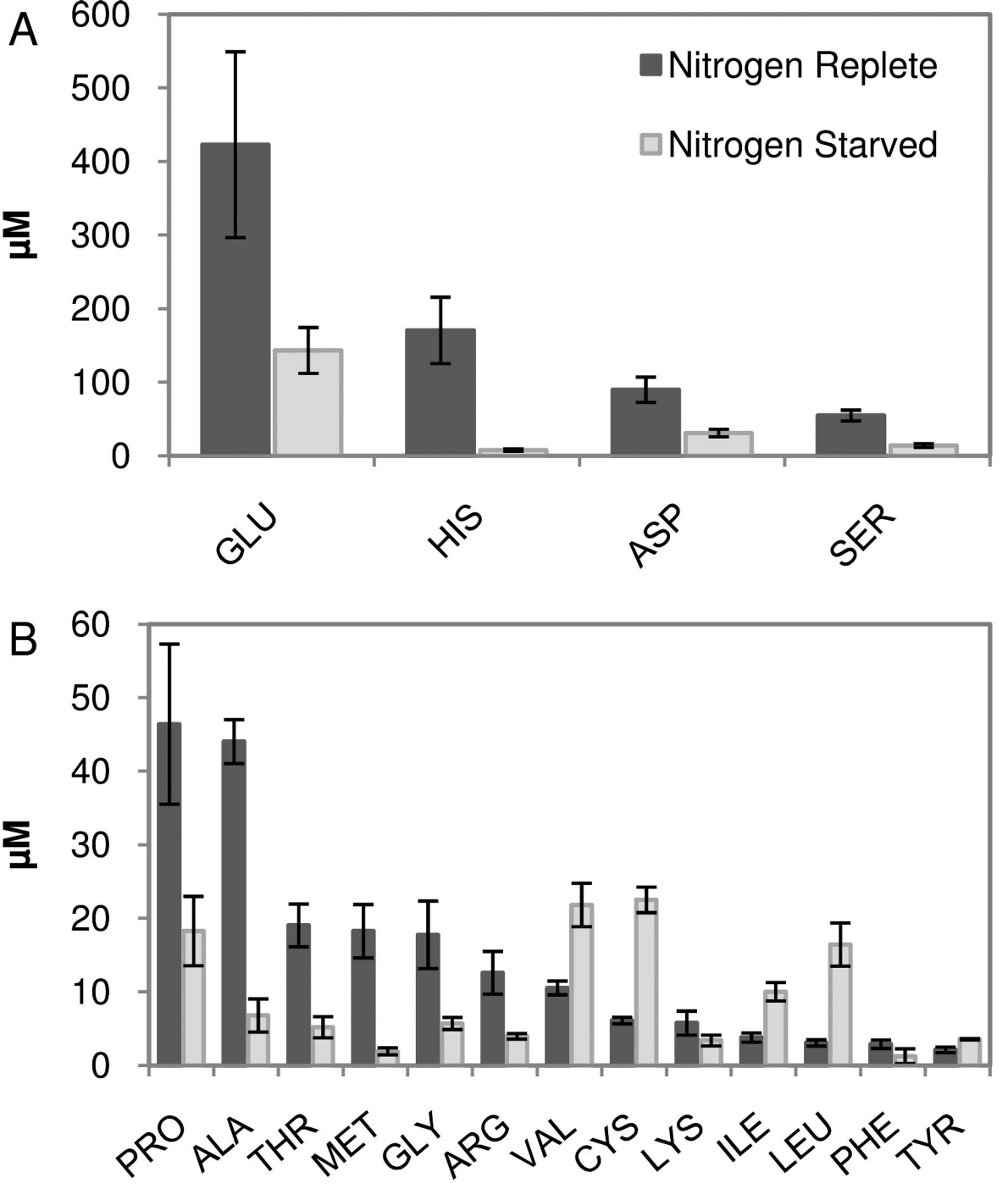

Figure 5. Intracellular concentration of individual amino acids in nitrogen replete (550 µM nitrate) and nitrogen starved (30 µM nitrate) *T. pseudonana* cells. A. The most abundant and B. the least abundant amino acids were determined by HPLC. Results are shown as means of 3 biological replicates ± standard deviation.

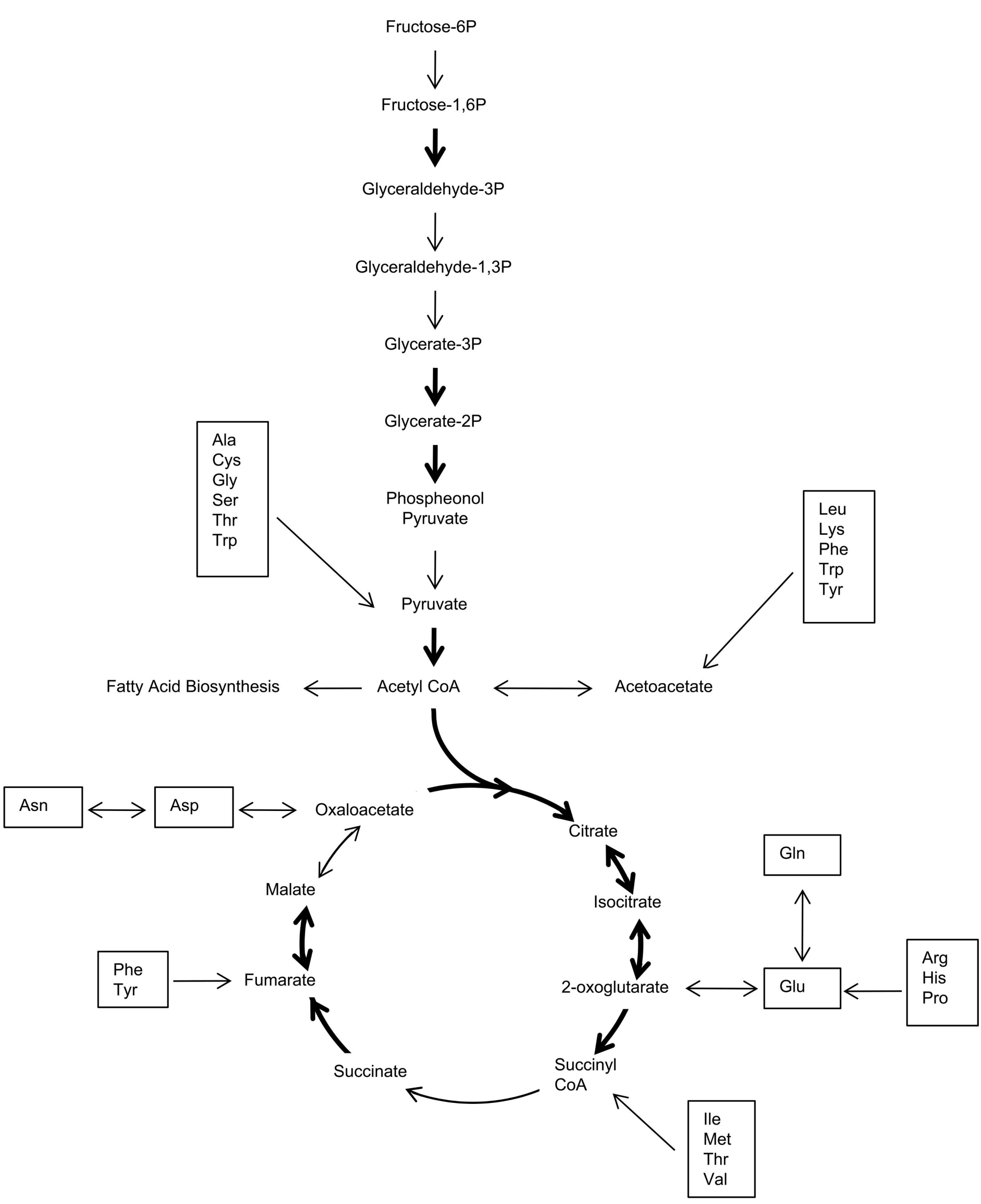

Figure 6. Representation of the changes in the abundance of proteins associated with carbon metabolism in *T. pseudonana* at the onset of nitrogen starvation. Increases are shown by bold arrows and no decreases were seen. Boxes show where carbon skeletons from amino acid degradation feed into the pathway.

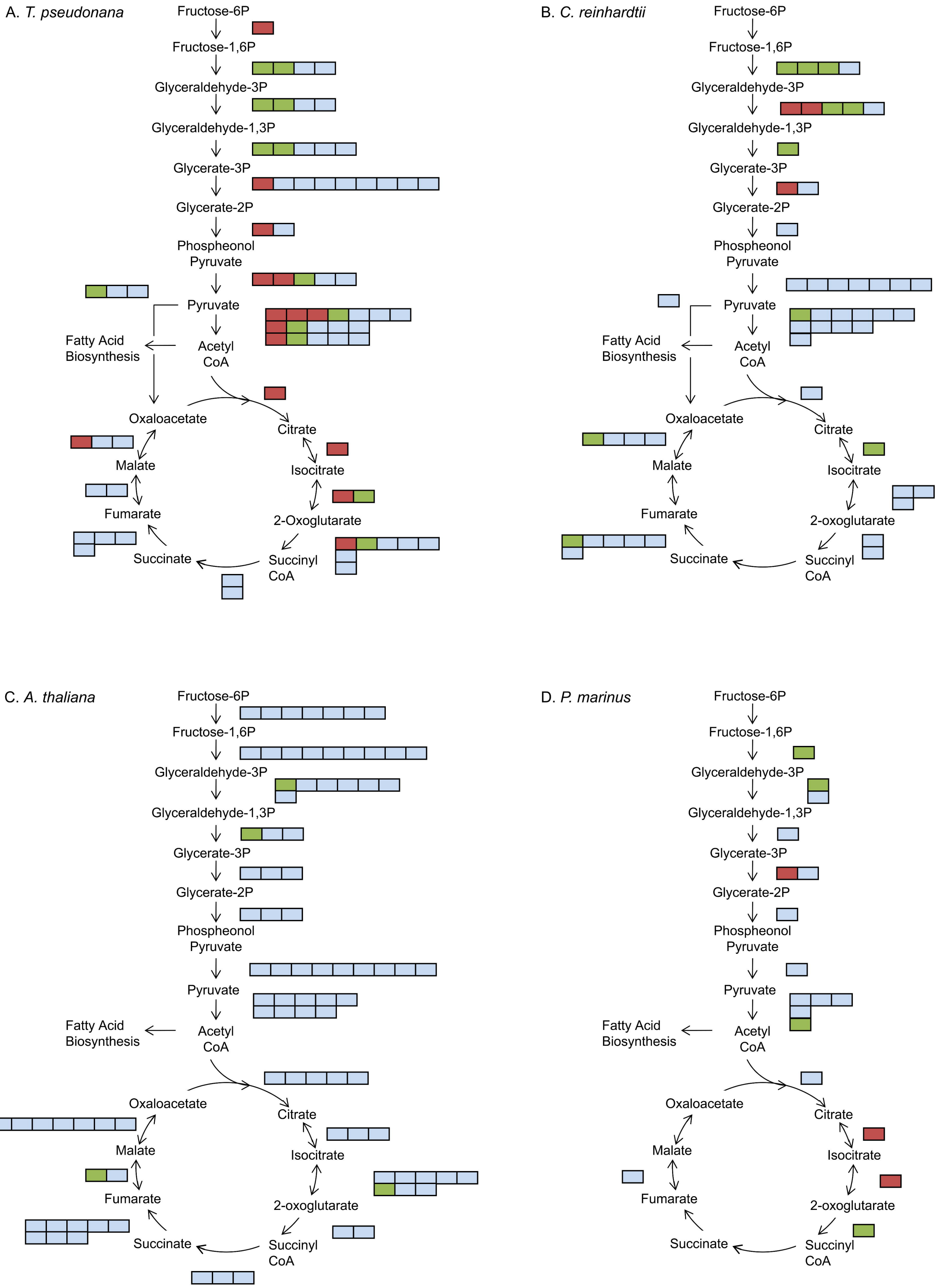

Figure 7. A comparison of changes in transcript levels associated with nitrogen deprivation in A. *T. pseudonana*, grown under conditions comparable to the current study(Mock et al 2008). B. *C. reinhardtii*, 48 h after the transfer of cells from 10 mM ammonium to nitrogen free medium.(Miller et al 2010). C. *A. thaliana*, at the onset of nitrogen limitation in plants grown with 3 mM nitrate (Peng et al 2007). D. *P. marinus* (MED4), 24 h after transfer from 800 µM ammonium into nitrogen free medium (Tolonen et al. 2006). Genes for each enzyme were identified using the genome databases for each species (*T. pseudonana*: http://genome.jgi-psf.org/Thaps3/Thaps3.home.html; *C. reinhardtii*: http://genome.jgi-psf.org/Chlre4/Chlre4.home.html; *A. thaliana*: www.arabidopsis.org; *P. marinus*: http://img.jgi.doe.gov/cgi-bin/w/main.cgi) and these were searched against the expression profiles presented in the four publications above to identify the degree of change in transcript level. Each box represents an isoform and multiple rows show that there is more than one enzyme responsible for a specific step. See Supplemental Table 2 for EC numbers and accession numbers. Red shows that transcript increased, green shows a decrease and blue shows stable transcript level.